Mass, Heat, and Momentum Transfer in the Flow of Gases Past Single Spheres

YIN-CHAO YEN and GEORGE THODOS

The Technological Institute, Northwestern University, Evanston, Illinois

The transfer of mass, heat, and momentum past a single sphere, 2.02 in. in diameter, was experimentally investigated for the turbulent flow of air between N_{Re} = 1,750 and N_{Re} = 8,922. The data resulting for the vaporization of water from the spherical surface verify the existence of the analogy between mass and heat transfer.

Measurements were made to account for the total drag and form drag of the sphere. The total drag was obtained by directly accounting for the force exerted, while the form drag was determined from static pressure measurements around the surface of the sphere. The resulting friction factors for total drag f and for form drag f_p were found to be of the same order of magnitude, thus making it impossible to account for the friction factor due to shear drag at these Reynolds numbers. Consequently it is not possible to determine if the analogy between mass and heat transfer can be extended to include the transfer of momentum for flow past single spheres at these conditions, although the results of this study cast considerable doubt on such an extension of this analogy.

The heat and momentum transfer analogy for the flow of fluids through circular conduits developed by Colburn (*2*) and extended by Chilton and Colburn (*1*) to mass transfer for these systems has utilized dimensionless j factors to relate the significant variables of each transfer process. This analogy has found widespread use in establishing these three modes of transfer in the flow of fluids through such circular ducts as wetted wall columns. However the extension of this analogy to the flow of gases through packed beds has been limited to mass and heat transfer only. In 1943 Gamson, Thodos, and Hougen (*5*) concluded from their experimental studies of the evaporation of water from porous catalyst carriers that an essentially direct correspondence exists between mass and heat transfer and that no analogy for momentum transfer was apparent from pressure-drop measurements taken across the packed bed.

In 1950 Sherwood (*11*) studied the three transfer processes for the turbulent flow of air past single cylinders. In this study the mass and heat transfer data of Powell (*10*), Lorisch (*7*), and Maisel and Sherwood (*8*) and the friction data compiled by Goldstein (*6*) were utilized. As a result Sherwood found that an analogy exists between mass, heat, and momentum transfer for the flow of fluids transverse to cylindrical surfaces when the friction factors utilized represented its shear drag contribution only.

An attempt to relate the transfer of heat and momentum for the flow of air past single spheres utilizing experimental heat transfer data is reported by Tang, Duncan, and Schweyer (*12*). The friction factor due to the total shear drag tangential to the surface f'_s was calculated with the Navier-Stokes equations and related to the Reynolds number in the laminar region between N_{Re} = 50 and N_{Re} = 1,000 by the use of the Reynolds analogy $(h)/(c_pG) = (f_s)/(2)$. Their resulting relationship can be expressed as follows:

$$\frac{f'_s}{2} = \frac{0.66}{N_{Re}^{0.50}} \qquad (1)$$

In the present investigation an attempt has been made to develop an analogy for mass, heat, and momentum transfer for the flow of air past single spheres utilizing for momentum only the shear drag portion obtained as the difference of total drag and form drag measurements in the direction of flow.

EXPERIMENTAL EQUIPMENT AND PROCEDURE

The experimental unit consisted of a vertical wind tunnel 14 in. in diameter and 26 ft. long, connected at its bottom to the intake end of a blower. Two parallel perforated steel plates, 6 in. apart, were provided at the top of the duct to establish uniform air velocities as the air was drawn downward into the tunnel. The flow of air was regulated with a sliding window near the suction end of the blower which permitted the variation of velocities in the wind tunnel from 1.8 to 9.5 ft./sec. The velocity of the air was measured with a pitot tube located 2 ft. above the test section and connected to a micromanometer. The test section was situated 10 ft. below the duct inlet and was provided with a sliding window to facilitate the introduction of test objects.

Total Drag Measurements

Exact spheres 2.02 in. in diameter were made identically from a catalyst carrier. A test sphere was supported on a stainless steel hollow rod which was inserted in a short threaded tap drilled along a major diameter. The rod was bent at a right angle, 3½ in. below the sphere, and extended horizontally to connect with the left beam of a balance through an aluminum adaptor. A diagrammatic sketch of the equipment is presented in Figure 1.

In order to counterbalance the weight of the sphere and its support a similar hollow rod extension of the right beam was mounted with an adjustable counterweight. To adjust the center of gravity of the balance a sliding brass weight was attached to the point indicator, and its position was varied until the balance would swing freely with reproducible results. To damp out oscillations resulting from the flow of air past the sphere and to detect the reaction of small forces acting on the sphere the end of the right beam extension was connected to the end of a light spring submerged in an oil bath. The small effect of the forces was detected by observing through a cathetometer the reflection of an illuminated scale from a small mirror, 0.8 cm. in diameter, positioned vertically on the side of the center of the beam. The illuminated scale and cathetometer were essentially adjacent to each other, 10¾ ft. from the mirror of the balance.

With the sphere mounted and the counter- and indicator-weights properly positioned a null point reading of the illuminating scale was taken through the cathetometer. Weights of the order of milligrams were placed on top of the sphere, and the beam deflection noted through the cathetometer served to establish the entire calibration curve. This technique provided means for measuring accurately the action of the small forces acting on the sphere.

Yin-chao Yen is with the Cold Regions Research and Engineering Laboratory, Corps of Engineers, Wilmette, Illinois.

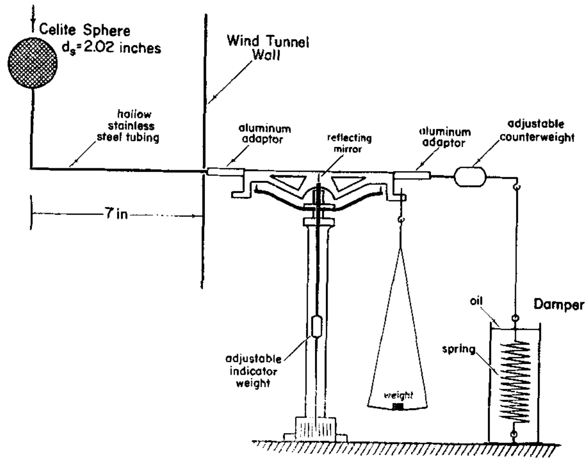

Fig. 1. Experimental equipment for mass, heat, and total momentum transfer studies in the flow of air past a single sphere.

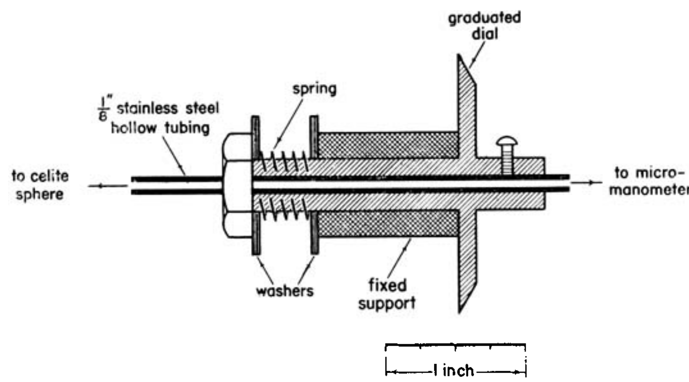

Fig. 2. Schematic diagram of sphere support for form-drag measurements.

The force contribution of the rod supporting the sphere was accounted for by suspending from the walls of the duct a similar sphere which was provided at the bottom with an opening in which the vertical end of the rod support would move in and out freely. With this arrangement a flow pattern of air was realized which was comparable to that obtained when the rod was fixed in the sphere. By applying this technique the forces acting on the rod support were measured for the velocity ranges of this study and subtracted from the previous measurements to obtain the forces acting on the sphere alone.

Mass and Heat Transfer Measurements

The same sphere utilized for total drag measurements was used in the simultaneous mass and heat transfer studies. A thermocouple wire (No. 40 gauge copper constantan) was permanently attached to the sphere surface by drilling a small hole through the vertical major diameter and inserting the wire through this hole so that the couple junction reached a point just below the opposite surface. The leads of the thermocouple were wrapped around the hollow support and then were connected to a potentiometer to record temperatures on the surface of the sphere. The temperature was measured only at the forward stagnation point of the sphere, since in the earlier work of Evnochides and Thodos (*4*) on the evaporation of water from celite spheres no significant temperature gradient around the sphere was noted at turbulent flow conditions.

The sphere was saturated with distilled water and subjected to drying by forcing past it air at room conditions. The temperature of the air flowing past the sphere was measured with two thermocouples located horizontally in the free stream. The loss in weight of the sphere during the constant drying rate period was determined by periodically removing weights from the balance pan to keep the beam always close to a neutral position. Final weight measurements were then made by stopping the flow of air and observing the exact position of the illuminated scale through the cathetometer. Approximately 30 sec. were required to make these weight measurements, while 15 to 20 min. constituted average time intervals between weighings.

Form Drag Measurements

The static pressure prevailing on the surface of the sphere was measured with a micromanometer. These measurements were conducted on a prepared sphere which was drilled with a ⅛-in. drill to the center of the sphere on two perpendicular major diameters. The threaded end of a stainless steel hollow tube, ⅛ in. in diameter, was inserted at one of the tapped openings of the sphere, providing a means for supporting the sphere horizontally, as shown in Figure 2.

The sphere support consisted of a fixed base in which could rotate a sleeve and a graduated dial which clamped in place the stainless steel tube with a set screw. With this arrangement the rotation of the dial caused the open end of the sphere to generate a great circle. To prevent the sphere from rotating freely a strong spring was provided which held the graduated dial tightly against the base support.

Pressure differences between the open end of the sphere and a reference point on the wall of the duct, approximately 6 in. above the sphere, were measured with the micromanometer. The micromanometer was capable of detecting pressure differences of 0.0001 in. of manometer fluid (isobutyl alcohol).

MASS AND HEAT TRANSFER

Twenty-nine experimental runs were conducted in order to establish the simultaneous mass and heat transfer from the surfaces of single spheres. The basic experimental data of typical runs are presented in Table 1. These data were analyzed with methods described elsewhere (*5, 10*) to produce the mass transfer factor j_d and the heat transfer factor j_h:

Table 1. Summary of Experimental Results and Calculated Values

Run no.	π, mm. Hg.	Test Section t_a, °F.	t_s, °F.	p_a, mm.	$r \times 10^3$ lb. water/hr.	q	k_g	h	j_d	j_h	N_{Re}
1	744.5	89.7	74.7	17.47	6.565	6.053	0.713	4.63	0.0100	0.0111	5,200
3	748.3	95.6	78.0	18.94	8.035	7.360	0.708	4.76	0.0097	0.0107	5,310
5	747.0	89.5	78.1	20.75	3.115	2.639	0.399	2.53	0.0158	0.0172	2,243
7	744.0	88.0	77.5	20.65	2.856	2.448	0.407	2.64	0.0161	0.0183	1,847
9	744.3	89.1	77.2	19.91	6.915	6.343	0.865	6.04	0.0073	0.0085	8,625
11	744.2	86.9	75.3	18.86	5.920	5.550	0.848	5.40	0.0084	0.0089	7,380
13	743.4	89.2	75.0	17.82	7.560	7.099	0.868	5.70	0.0088	0.0093	7,375
15	743.4	84.2	74.5	18.72	4.890	4.600	0.795	5.41	0.0086	0.0098	6,720
17	742.2	86.1	76.8	21.68	3.295	2.910	0.561	3.57	0.0114	0.0120	3,613
19	743.0	85.2	73.2	17.01	4.170	3.751	0.547	3.56	0.0117	0.0127	3,430
21	746.9	89.6	67.4	10.24	6.205	5.388	0.434	2.76	0.0142	0.0149	2,155
23	754.2	85.0	64.1	8.72	5.980	5.262	0.439	2.87	0.0129	0.0153	2,285
25	755.1	80.1	66.5	12.24	5.190	3.767	0.471	3.26	0.0132	0.0144	2,690
27	743.5	78.9	66.3	12.71	3.860	3.442	0.480	3.11	0.0134	0.0140	2,730
29	745.7	77.8	60.9	8.36	5.145	4.513	0.482	3.01	0.0117	0.0120	3,165

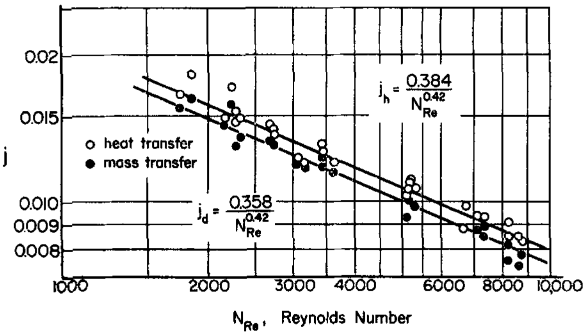

Fig. 3. Relationships between heat and mass transfer factors and Reynolds number for single sphere.

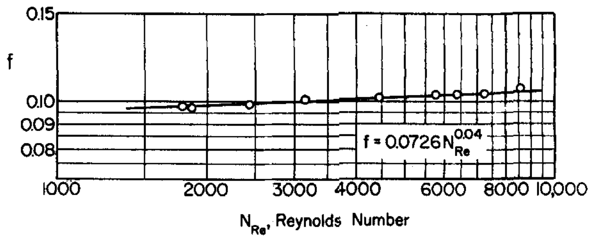

Fig. 5. Relationship between friction factor and Reynolds number.

$$j_d = \frac{k_g\, p_{sf}}{G/M_m}\left(\frac{\mu}{\rho\, D_v}\right)_f^{2/3} \qquad (2)$$

and

$$j_h = \frac{h}{c_p\, G}\left(\frac{c_p\, \mu}{k}\right)_f^{2/3} \qquad (3)$$

In the calculation of these factors the Schmidt and Prandtl groups were found to be essentially constant, having the average values $N_{Sc} = 0.606$ and $N_{Pr} = 0.719$.

Radiation effects from the surroundings and conduction through the support of the sphere were accounted for in the calculation of h. The temperature on the surface of the sphere was always found to be slightly higher than that expected from wet-bulb thermometry, in agreement with the conclusions of DeAcetis and Thodos (3) for the flow of air through packed beds of wet spheres.

The resulting mass and heat transfer factors j_d and j_h are plotted vs. the Reynolds number in Figure 3. The resulting relationships can be expressed as follows:

$$j_d = \frac{0.358}{N_{Re}^{0.42}} \qquad (4)$$

$$j_h = \frac{0.384}{N_{Re}^{0.42}} \qquad (5)$$

These factors are consistent with the transfer factors reported by Maisel and Sherwood (8) and McAdams (9) for flow past single spheres. The ratio $j_h/j_d = 1.073$ is in close agreement with the value 1.076 reported by Gamson, Thodos, and Hougen (5) for the flow of air through packed beds of wet particles.

MOMENTUM TRANSFER

Fifty-six runs for ten different Reynolds numbers were conducted to obtain information on the total drag force exerted by the air on the sphere and support. In addition forty-three runs for seventeen different Reynolds numbers were conducted to determine the drag force on the support alone. The values of the two sets of drag forces are plotted in Figure 4 vs. Reynolds number. The drag force on the sphere was obtained as the difference between the two measurements at a given Reynolds number.

The drag force of a fluid F exerted on a sphere can be related to the area of the sphere and the kinetic energy of the fluid flowing past the surface as follows:

$$F = f(\pi D_s^2)\,\frac{\rho u^2}{2g_c} \qquad (6)$$

where f includes contributions due to the pressure distribution over the surface and shear effects caused by velocity gradients on the spherical surface:

$$f = f_p + f_s \qquad (7)$$

Equation (6) was used to calculate the friction factor for each of the ten different Reynolds numbers. The friction factor is plotted against the Reynolds number in Figure 5. The resulting relationship for $1{,}768 < N_{Re} < 8{,}575$ can be expressed as follows:

$$f = 0.0726\, N_{Re}^{0.04} \qquad (8)$$

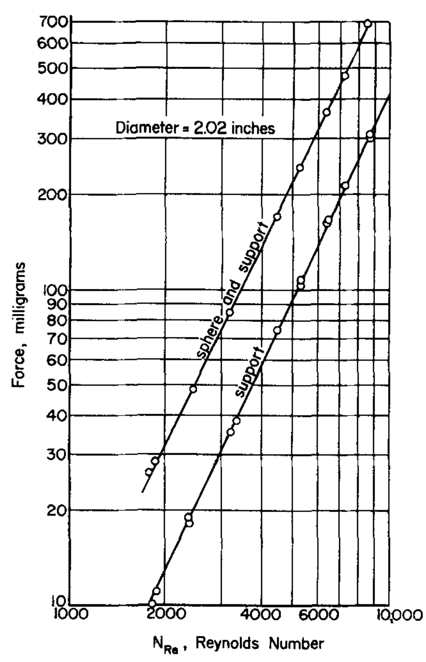

Fig. 4. Drag force on sphere and support and on support alone vs. Reynolds number.

Equation (8) produces values that are essentially consistent with those reported by Wieselberger (13) for spheres varying from 18.0 to 282.5 mm. in diameter.

The static pressure distribution around the surface of the sphere, determined by measuring the difference between the static pressure at a point on the surface of the sphere and at a reference point upstream in the vertical wind tunnel, was used to determine f_p. Fifteen experimental runs were conducted covering Reynolds numbers ranging from 2,435 to 8,922.

For a fluid flowing past a single sphere of radius R the force due to form drag over the entire surface of the sphere is given by

$$F_p = \int_0^{2\pi}\int_0^{\pi} (P_\vartheta - P_\infty) R^2 \sin\vartheta \cos\vartheta\, d\vartheta\, d\varphi \qquad (9)$$

where $R^2 \sin\vartheta \cos\vartheta\, d\vartheta\, d\varphi$ represents a differential element of the spherical surface. Since in the present investigation axial symmetry exists, Equation (9) reduces to

$$F_p = \pi R^2 \int_0^{\pi} (P_\vartheta - P_\infty)\, d(\sin^2\vartheta) \qquad (10)$$

By analogy to Equation (6) the force due to form drag can also be expressed as

$$F_p = f(4\pi R^2)\,\frac{\rho u^2}{2g_c} \qquad (11)$$

When one combines Equations (10) and (11), the friction factor due to form drag becomes

$$f_p = \frac{1}{4}\int_0^{\pi} \frac{P_\vartheta - P_\infty}{\rho u^2/2g_c}\, d(\sin^2\vartheta) \qquad (12)$$

The dimensionless quantity $(P_\vartheta - P_\infty)/\rho u^2)/(2g_c)$ was plotted against $\sin^2\vartheta$ for all fifteen runs. The results of a typical run (Run 7) are presented in Figure 6. It is possible to show that the integral of Equation (12) is equal to the area abc plus the area $acgef$ minus the area $cdeg$, between the limits $\vartheta = 0$ and $\vartheta = \pi$. For Run 7 f_p was found to be $\frac{1}{4}(0.4232) = 0.1058$. Table 2 presents a summary of the form drag friction factors along with other basic information including Reynolds numbers for the fifteen experimental runs. For each Reynolds number the total friction factor was calculated from Equation (8). In the majority of cases the friction factor due to form drag, was found to be of the same order of magnitude as the friction factor due to total drag. Thus the friction factor due to shear drag could not be accurately established as the difference between f and f_p. As a matter of fact f_s was found to be positive only for low Reynolds numbers. Therefore at these conditions the friction factor due to shear drag cannot be used in an attempt to extend the analogy for mass and heat transfer to include momentum transfer for flow past single spheres, unless considerably more exacting drag measurements could be made.

If the analogy for momentum is assumed to apply, then $f_s = 2j$. In the range of conditions investigated in this study the extreme values of f_s to be expected from Equation (4) are $f_s = 0.0270$ for $N_{Re} = 2{,}435$ and $f_s = 0.0158$ for $N_{Re} = 8{,}795$. However a shear drag friction factor of this order of magnitude is not probable from the results of this study, since the form drag friction factors would have to be much smaller than those obtained. For example at $N_{Re} = 5{,}384$ the value of f_p would have to be $0.1025 - 0.0194 = 0.0831$, as opposed to the value $f_p = 0.1020$ actually obtained. An error of 18.5% in the calculation of f_p is highly unlikely.

In view of these findings no analogy appears to exist between momentum and mass and heat transfer for the flow of fluids past single spheres with only the friction factor due to shear drag. In the range of Reynolds numbers $N_{Re} = 2{,}435$ to $N_{Re} = 8{,}795$ the friction factor due to shear drag is too small to be determined accurately as the difference between the total friction factor and the friction factor due to form drag. Since the friction factor due to shear drag increases with decreasing Reynolds number, it would be advisable to make the necessary modifications of the equipment so that friction factors due to shear drag at lower Reynolds numbers could be determined.

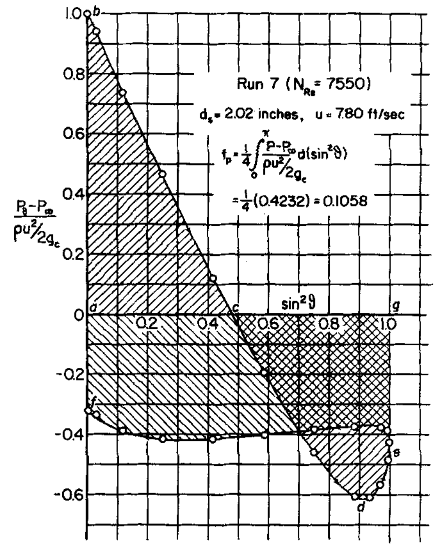

Fig. 6. Graphical integration to determine the friction factor due to form drag in the flow of air past a single sphere.

NOTATION

A	=	total area of sphere, sq. ft.
c_p	=	heat capacity, B.t.u./lb.-mass °F.
d_s	=	diameter of sphere, in.
D_s	=	diameter of sphere, ft.
D_v	=	diffusion coefficient, sq. ft./hr.
f	=	friction factor due to shear and form drag, based on total area, $f_p + f_s$
f_p	=	friction factor due to form drag, based on total area of sphere
f_s	=	friction factor due to shear drag, based on total area of sphere
f_s'	=	friction factor due to total shear drag tangential to sphere surface
F	=	total force due to shear and form drag in direction of flow, $fA(\rho u^2)/(2g_c)$
F_p	=	total force due to form drag in direction of flow, $f_pA(\rho u^2)/(2g_c)$
g_c	=	conversion factor, 32.17 lb.-mass ft./lb.-force sec.^{2}
h	=	heat transfer coefficient, B.t.u./hr. sq. ft. °F.
G	=	mass velocity, lb.-mass/hr. sq. ft.
k	=	thermal conductivity, B.t.u./hr. ft. °F.
k_g	=	mass transfer coefficient, lb.-moles/hr. sq. ft. atm.
j_d, j_h	=	transfer factors for mass and heat, respectively
M_m	=	average molecular weight
p_a	=	partial pressure of water in air stream
p_s	=	vapor pressure of water on surface of sphere
p_{gf}	=	average partial pressure of nontransferable component in gas film, atm.
P_ϑ	=	static pressure on surface of sphere at angle ϑ from forward point of stagnation, atm.
P_∞	=	static pressure of undisturbed stream, atm.
q	=	rate of heat flow, B.t.u./hr.
r	=	rate of mass transfer, lb.-moles/hr.
r, ϑ, φ	=	spherical coordinates
R	=	radius of sphere, ft.
N_{Pr}	=	Prandtl number, $(c_p\mu)/(k)$
N_{Re}	=	Reynolds number for spheres, $(D_s u\rho)/(\mu)$
N_{Sc}	=	Schmidt number, $(\mu)/(\rho D_v)$
t_a	=	dry bulb temperature of air in test section, °F.
t_s	=	surface temperature of sphere, °F.
u	=	velocity of undisturbed stream, ft./sec.
π	=	atmospheric pressure
π	=	constant, 3.1416
μ	=	absolute viscosity, lb.-mass/sec. ft.
ρ	=	density, lb./cu. ft.

TABLE 2. SUMMARY OF CALCULATED FRICTION FACTORS DUE TO FORM DRAG AND THE COMPARISON OF THESE WITH TOTAL FRICTION FACTORS AT CORRESPONDING REYNOLDS NUMBERS

$d_s = 2.02$ in.

Run	t, °F.	π, mm. Hg.	N_{Re}	f	f_p	f_s
1	82.5	747.5	2,435	0.0991	0.0999	
2	82.5	747.4	3,275	0.1002	0.0883	0.0119
3	82.5	746.9	3,731	0.1008	0.0928	0.0080
4	80.7	751.0	4,651	0.1020	0.1007	0.0013
5	80.0	748.2	5,384	0.1025	0.1020	0.0005
6	80.4	745.8	6,282	0.1035	0.1045	
7	80.5	746.5	7,550	0.1045	0.1058	
8	80.5	745.7	8,922	0.1050	0.1049	0.0001
9	85.0	751.5	2,429	0.0990	0.0844	0.0146
10	85.2	749.3	3,624	0.1007	0.1024	
11	89.0	745.2	4,424	0.1015	0.1050	
12	88.0	745.0	5,102	0.1023	0.1143	
13	84.3	745.2	6,210	0.1035	0.1105	
14	84.5	744.2	7,408	0.1042	0.1086	
15	84.7	748.2	8,795	0.1048	0.1127	

LITERATURE CITED

1. Chilton, T. H., and A. P. Colburn, *Ind. Eng. Chem.*, **26**, 1183 (1934).
2. Colburn, A. P., *Trans. Am. Inst. Chem. Engrs.*, **29**, 174 (1933).
3. De Acetis, James, and George Thodos, *Ind. Eng. Chem.*, **52**, 1003 (1960).
4. Evnochides, Spyros, and George Thodos, *A.I.Ch.E. Journal*, **7**, 78 (1961).
5. Gamson, B. W., George Thodos, and O. A. Hougen, *Trans. Am. Inst. Chem. Engrs.*, **39**, 1 (1943).
6. Goldstein, S., "Modern Developments in Fluid Mechanics," p. 496, Oxford Univ. Press, London, England (1938).
7. Lorisch, W., *Mitt. Forsch.*, **322**, 46 (1929).
8. Maisel, D. S., and T. K. Sherwood, *Chem. Eng. Progr.*, **46**, 131 (1950).
9. McAdams, W. H., "Heat Transmission," 2 ed., p. 236, McGraw-Hill, New York (1942).
10. Powell, R. W., *Trans. Inst. Chem. Engrs. (London)*, **18**, 36 (1940).
11. Sherwood, T. K., *Ind. Eng. Chem.*, **42**, 2077 (1950).
12. Tang, Y. S., J. M. Duncan, and H. E. Schweyer, *Natl. Advisory Comm. Aeronaut. Tech. Note* 2867 (March, 1953).
13. Wieselberger, C., *Ergeb. Aerodyn. Versuchanstalt Göttingen*, **2**, 22 (1923).

Manuscript received November 22, 1960; revision received May 15, 1961; paper accepted May 17, 1961.

An Experimental Study of Three Component Gas Diffusion

J. B. DUNCAN and H. L. TOOR

Carnegie Institute of Technology, Pittsburgh, Pennsylvania

Equimolal countercurrent diffusions runs were made in a two bulb diffusion cell with the system hydrogen, nitrogen, and carbon dioxide. The initial bulb compositions were chosen so that various types of ternary interactions occurred. These interactions were well-described by the Maxwell-Stefan equations. The average deviation of the experimental mole fractions for all runs from those predicted by the Maxwell-Stefan equations was 0.45 mole %.

The differential equations describing isothermal, isobaric diffusion in ideal gas mixtures, the Maxwell-Stefan equations (*11, 12*), have been known for a long time. Various integrations for steady state unidirectional diffusion without reaction in three component gas mixtures have been presented. Gilliland considered diffusion with one gas stagnant (*18*), special cases of interest in the analysis of stagewise diffusional have been considered (*1, 2*), and Hoopes (*8*), as well as Keys and Pigford (*10*), presented solutions with the rates of transfer unrestricted. Hellund, who did not start with the Maxwell-Stefan equations, considered an unsteady state diffusion problem (*5, 6*). Hougen and Watson (*9*) and Wilke (*22*) developed approximate multicomponent solutions based on effective diffusivities, and Stewart presented an alternate method of computing effective diffusivities (*14*).

A solution for equimolal countercurrent diffusion, with simple approximate solutions, has been presented (*19*). The predicted behavior was found to be quite different from the behavior of corresponding binary systems. Even though the mean velocity is zero, the flux of a component may be zero in the presence of a concentration gradient of that component, a flux may exist in the absence of a gradient, or the direction of transfer may be against the concentration gradient of that component. (From the viewpoint of irreversible thermodynamics these are cross-diffusion effects.)

This behavior may be considered to be a consequence of the addition of a third component to what was originally a binary mixture and the above phenomena classed as ternary interaction phenomena. These are conveniently described as a diffusion barrier (*19*), osmotic diffusion (*5, 6*), and reverse diffusion (*19*) respectively. (Because the addition of further components to the three component mixture introduces no new effects, these interactions may also be considered to be multicomponent interaction phenomena.)

The first effect corresponds to zero values of the above mentioned effective diffusion coefficient, the second to singularities, and the third to negative values. The effective diffusivities of Wilke* and Stewart show this behavior but Hougen and Watson's do not (*21*). Further analysis indicated that these interaction phenomena could drastically affect design calculations, plate efficiencies for example (*20*). Recent work has shown that the above phenomena do occur in ternary mass transfer (*17*).

Papers reporting experimental work in diffusion of ternary gas mixtures are not numerous. In a few the validity of the Maxwell-Stefan equations is investigated. Fairbanks and Wilke (*4*) studied diffusion of one gas through two stagnant gases and showed that the results were in agreement with Wilke's approximate solution of the Maxwell-Stefan equations (*22*).

Keyes and Pigford investigated the separation of a binary gas mixture by passing a third gas through the mixture (*10*), and Hoopes measured both fluxes and gradients in a system in which all three fluxes were related to each other by a chemical reaction

J. B. Duncan is with Monsanto Chemical Company, St. Louis, Missouri.

* Wilke's method 2 modified as suggested by Toor (*19*). Wilke's method 1 does not have the proper behavior.